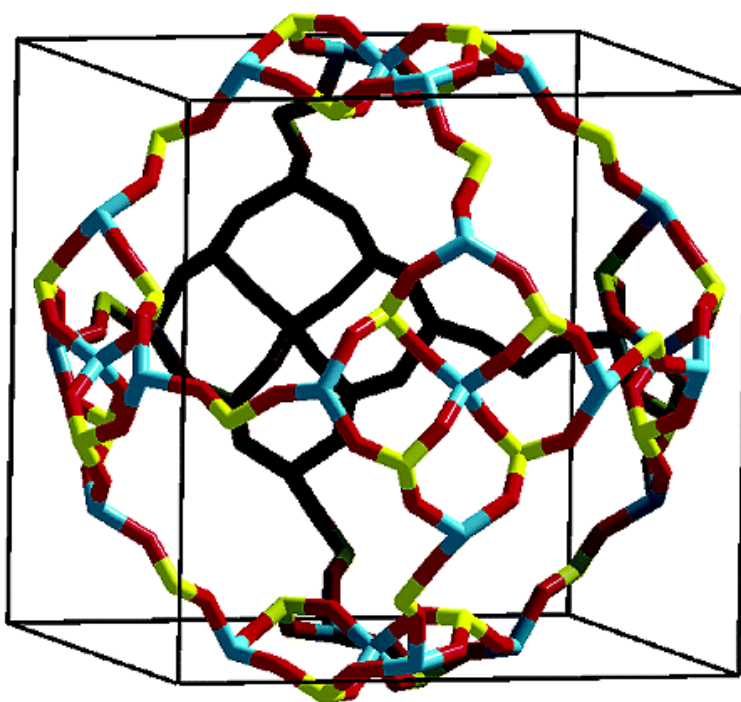Article

Order–Disorder in the Super-Sodalite ZnAl(PO), 4*tren*, 17HO (MIL-74): A Combined XRD–NMR Assessment

Lionel Beitone, Clarisse Huguenard, Axel Gansmller, Marc
Henry, Francis Taulelle, Thierry Loiseau, and Grard Frey

More About This Article

Additional resources and features associated with this article are available within the HTML version:

- Supporting Information
- Links to the 8 articles that cite this article, as of the time of this article download
- Access to high resolution figures
- Links to articles and content related to this article
- Copyright permission to reproduce figures and/or text from this article

Order−Disorder in the Super-Sodalite Zn$_3$Al$_6$(PO$_4$)$_{12}$, 4*tren*, 17H$_2$O (MIL-74): A Combined XRD−NMR Assessment

Lionel Beitone,[†] Clarisse Huguenard,[§] Axel Gansmüller,[§] Marc Henry,[§]
Francis Taulelle,[§] Thierry Loiseau,*,[†] and Gérard Férey[†,‡]

Contribution from the Institut Lavoisier (UMR CNRS 8637) and Institut Universitaire de France, Université de Versailles St Quentin en Yvelines, 45, Avenue des Etats Unis, 78035 Versailles, France, and Tectonique Moléculaire du Solide FRE 2423, Université Louis Pasteur, 4 rue Blaise Pascal, 67000 Strasbourg, France

Received November 26, 2002; E-mail: loiseau@chimie.uvsq.fr

Abstract: A new mixed zinc−aluminum phosphate Zn$_3$Al$_6$(PO$_4$)$_{12}$, 4*tren*, 17H$_2$O (MIL-74) has been hydrothermally synthesized with the tris(2-aminoethyl)amine (*tren*) as a structure-directing agent (453 K, 36 h, autogenous pressure). The solid was characterized by a nonclassical method combining single-crystal X-ray diffraction and several solid-state NMR experiments, RFDR, C7 double quantum (^{31}P), and 3QMAS (^{27}Al). Its crystal structure is cubic, $a = 16.7942(1)$ Å, but the choice of the space group does not follow usual routes of structure determination, due to some "disorder" between Zn and Al. It can be assigned as well to *I*-43*m* or to *P*-43*n*. The open-framework is built up from an enneameric unit (T = Zn, Al) containing five TO$_4$ and four PO$_4$ tetrahedra (one of the P−O bonds is terminal). A central TO$_4$ tetrahedral unit shares all of the corners with four phosphates groups. Two phosphate groups are connected to two other peripheral TO$_4$ units. It results in the formation of a "pseudo" planar building block T$_5$P$_4$ consisting of four square 4-rings. The connection of the T$_5$P$_4$ units generates a three-dimensional framework, which defines a super-sodalite topology. The resulting cavities (diameter of 10 Å) are bound by 12-ring windows in which are located the *tren* species in interaction with the phosphate groups (mainly terminal P−O bonds) through hydrogen bonds. A cluster of 17 water molecules occupies the center of the super-sodalite cage. The cationic (Zn, Al) occupancy is discussed for this specific topology.

Introduction

In the domain of zeolite-related compounds,[1] one of the challenges is currently the discovery of solids with very large pores,[2] to enhance applications in catalysis, gas separation/storage, and to transform the pores into nanoreactors. The concept of scale chemistry[3] can be used for such a purpose. It originated from two facts: the observation within the hydro-thermal solution[4] of the oligomeric building units very close to those existing in the final solid and the dependence of the size of these units on the charge density of the template. The lower the charge density is, the larger are the bricks, and, therefore, the larger are the pores. This hypothesis was verified many times in our group on fluorinated gallophosphates[5] and can help in the search for new porous solids. In our group, ULM-5 and ULM-16, with 16-membered rings (MR), and MIL-31 and MIL-

46 with 18 MR are the best illustrations of this idea.[6] The size of the tunnels can even reach 24 MR[7] in a few cases.

This idea of scale chemistry can also be applied to the porous organically templated aluminum (AlPO-*n*) and gallium (GaPO-*n*) phosphates, first reported by Flanigen et al.[8] and Parise,[9] respectively. The fluorinated gallophosphate Cloverite,[10] obtained with quinuclidine as a template, is, a posteriori, an illustration of this concept. Our group has undertaken a systematic study of these systems. Our strategy[11] concerns both the use of large amines to decrease the charge density of the template and the introduction to some extent of mono- and divalent ions besides Al and Ga for increasing the initial negative

[†] Institut Lavoisier, Université de Versailles St Quentin en Yvelines.
[‡] Institut Universitaire de France, Université de Versailles St Quentin en Yvelines.
[§] Université Louis Pasteur.
(1) (a) Cheetham, A. K.; Férey, G.; Loiseau T. *Angew. Chem., Int. Ed.* **1999**, *38*, 3268. (b) Davis, M. E. *Nature* **2002**, *417*, 813. (c) Férey, G. *Chem. Mater.* **2001**, *13*, 3084. (d) Thomas, J. M. *Angew. Chem., Int. Ed.* **1999**, *38*, 3588. (e) Corma, A. *Chem. Rev.* **1995**, *95*, 559.
(2) Férey, G.; Cheetham, A. K. *Science* **1999**, *283*, 1125.
(3) Férey, G. *J. Solid State Chem.* **2000**, *152*, 37.
(4) Haouas, M.; Gérardin, C.; Taulelle, F.; Estournes, C.; Loiseau, T.; Férey, G. *J. Chim. Phys.* **1998**, *95*, 302. Taulelle, F.; Haouas, M.; Gérardin, C.; Estournes, C.; Loiseau, T.; Férey, G. *Colloids Surf., A* **1999**, *158*, 299.
(5) Férey, G. *C. R. Acad. Sci. Paris, Ser. IIc* **1998**, *1*, 1.

(6) (a) Loiseau, T.; Férey, G. *J. Solid State Chem.* **1994**, *111*, 403. (b) Loiseau, T.; Férey, G. *J. Mater. Chem.* **1996**, *6*, 1073. (c) Sassoye, C.; Loiseau, T.; Taulelle, F.; Férey, G. *Chem. Commun.* **2000**, 943. (d) Sassoye, C.; Marrot, J.; Loiseau, T.; Férey, G. *Chem. Mater.* **2002**, *14*, 1340.
(7) (a) Guillou, N.; Gao, Q.; Nogues, M.; Morris, R. E.; Hervieu, M.; Férey, G.; Cheetham, A. K. *C. R. Acad. Sci. Paris, Ser. IIc* **1999**, *2*, 387. (b) Guillou, N.; Forster, P. M.; Gao, Q.; Chang, J. S.; Nogues, M.; Park, S. E.; Cheetham, A. K.; Férey, G. *Angew. Chem., Int. Ed.* **2001**, *40*, 2831. (c) Yang, G. Y.; Sevov, S. C. *J. Am. Chem. Soc.* **1999**, *121*, 8389. (d) Lin, C.-H.; Wang, S.-L; Lii, K. H. *J. Am. Chem. Soc.* **2001**, *123*, 4649. (e) Zhou, Y.; Zhu, H.; Chen, Z.; Chen, M. *Angew. Chem., Int. Ed.* **2001**, *40*, 2166. (f) Plévert, J.; Gentz, T. M.; Laine, A.; Li, H.; Young, V. G.; Yaghi, O. M.; O'Keeffe, M. *J. Am. Chem. Soc.* **2001**, *123*, 12706.
(8) Wilson, S. T.; Lok, B. M.; Messina, C. A.; Cannan, T. R.; Flanigen, E. M., *J. Am. Chem. Soc.* **1982**, *104*, 1146.
(9) Parise, J. B. *Inorg. Chem.* **1985**, *24*, 4312.
(10) Estermann, M.; McCusker, L. B.; Baerlocher, C.; Merrouche, A.; Kessler, H. *Nature(London)* **1991**, *352*, 320.
(11) Férey, G. *J. Fluorine Chem.* **1995**, *72*, 187.

charge of the unit. It increases, therefore, the condensation of oligomers in solution up to the point where electronegativities of both the unit and the templates become equal.

Initially, the isomorphous substitution of Al^{3+} by divalent metal (Me^{2+}) cations (MeAPO; Me = Mg, Mn, Co, Zn, etc.) was described for the production of remarkable catalytic activity due to the negative charges on the $AlPO_4$ frameworks (generation of Brönsted acid sites).[12] A large number of mixed Al/Me phosphate-based materials with novel three-dimensional architectures have been prepared. Some of them exhibit extra-large pore structures with cavity diameters up to 20 Å.[13] The divalent metal must offer an ability to adopt a tetrahedral coordination for its incorporation in the $AlPO_4$ network. For that purpose, zinc is one of the candidates of choice, and many works reported its utilization in the formation of open-framework phosphates.[7c,14]

In this paper, a new phase $Zn_3Al_6(PO_4)_{12}$, 4*tren*, $17H_2O$ (MIL-74) obtained in the system $ZnO-Al_2O_3-P_2O_5-tren-H_2O$ (*tren* stands for tris(2-aminoethyl)amine) was synthesized under mild hydrothermal conditions. The main interest of this paper concerns the thorough structural study of the extent of cationic ordering between Zn and Al in this super-sodalite structure. Combined X-ray diffraction and solid-state NMR demonstrate their capabilities of pushing the limits of structural description well beyond what is usually expected, albeit at a cost: a demand for a much finer description of crystallographical features.

Therefore, the format of the paper is as follows: after the Experimental Section, the first part will be devoted to the classical X-ray diffraction study of the title compound and its crystal chemistry. The second part reports the NMR results on the solid and the partial misfit which exists between X-ray and NMR information. Finally, the extent of cationic order will be discussed.

Experimental Section

Hydrothermal Synthesis. A sample of $Zn_3Al_6(PO_4)_{12}$, 4*tren*, $17H_2O$ (MIL-74) was prepared under hydrothermal conditions. First, 4.16 g (2.3×10^{-1} mol) of purified water was added to 0.27 g (3.5×10^{-3} mol) of aluminum hydroxide powder $Al(OH)_3$, xH_2O (Al_2O_3 content 50−57%, Aldrich). Next, 0.52 g (1.7×10^{-3} mol) of zinc nitrate hexahydrate (Aldrich, 98%), 0.80 g (6.8×10^{-3} mol) of orthophosphoric acid, and 0.86 g (5.9×10^{-3} mol) of tris(2-aminoethyl)amine (*tren*, $N_4C_6H_{18}$, Aldrich 96%) were successively added to give a mixture of overall molar composition $0.5Al_2O_3$:$0.5ZnO$:$1P_2O_5$:$1.7tren$:$80H_2O$. The reactants were magnetically stirred for 5 min, sealed into a 23 mL Teflon-lined Parr bomb (filling rate 25%), and heated at 453 K for 36 h under autogenous pressure before cooling during 12 h to room temperature. The initial and final pH values were both ca. 10. The white powdered product was collected by filtration, washed with purified water, and dried at room temperature.

$Zn_3Al_6(PO_4)_{12}$, 4*tren*, $17H_2O$ (MIL-74) crystals suitable for single-crystal X-ray diffraction were obtained by the reaction of a mixture of overall composition $0.5Al_2O_3$:$0.5ZnO$:$0.5P_2O_5$:$1.9tren$:$80H_2O$. The reaction conditions were identical to those of the powdered product, except for the source of aluminum: another type of aluminum hydroxide was used (Al_2O_3 content 64.5−67%, Rectapur, Prolabo). This specific molar composition led to the formation of relatively large multifaceted crystals, but the unreacted aluminum source is still present with the
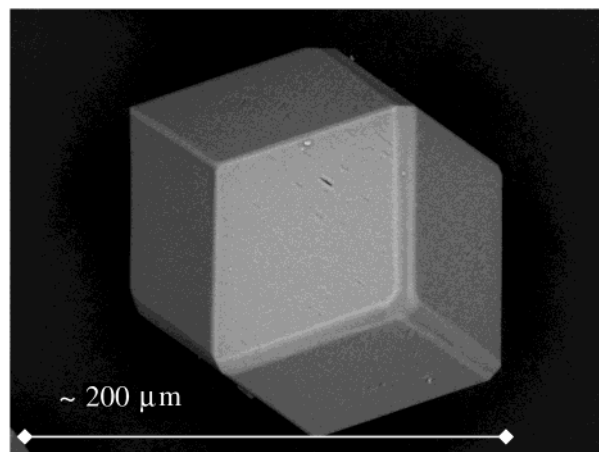

Figure 1. Dodecahedral rhombohedron of $Zn_3Al_6(PO_4)_{12}$, 4*tren*, $17H_2O$ (MIL-74), as observed by scanning electron microscopy (in size, 200 μm).

crystalline sample. The very nice crystals, observed by scanning electron microscopy (JEOL JSM-5800LV), have a shape of a rhombododecahedron (∼200 μm in size, Figure 1) consisting of 12 well-defined rhombic faces. The crystals have four three-fold axes and three four-fold axes, which are compatible with a symmetry belonging to the different point groups of the cubic class.

Elemental Analyses. Zn, Al, P, C, N, and H chemical analyses were performed by ICP emission spectroscopy at the National Center of Analysis of CNRS (Vernaison, France). The elemental analysis of the sample confirms the chemical formula of the title compound Zn_3Al_6-$(PO_4)_{12}$, 4*tren*, $17H_2O$ (weight %): Zn, 7.8 (calc. 8.2); Al, 6.3 (calc. 6.7); P, 15.2 (calc. 15.5); C, 12.2 (calc. 12.0); N, 9.5 (calc. 9.3); H, 5.0 (calc. 4.9).

Thermogravimetry. TGA measurements were obtained using a TGA 2500 thermogravimetric analyzer (TA Instruments) with a heating rate of 2 K min⁻¹ under O_2 atmosphere up to 1073 K. They reveal two weight losses. The first occurs between 293 and 547 K. It can be assigned to the departure of the 17 free water molecules (exp. 14.0 wt %; calc. 13.8 wt %). The second one begins at 547 K and is mainly due to the departure of the amine (exp. 19.9 wt %). The calculated value of the weight loss cannot be clearly assigned because the X-ray powder pattern of the residue is a mixture of $AlPO_4$ cristobalite (JCPDS file 11-0500), ZnP_2O_7 (JCPDS file 73-1648), and unknown phases.

X-ray Diffraction. The X-ray diffraction powder patterns were obtained using a D5000 Bruker diffractometer at room temperature ($\lambda_{Cu\ K\alpha}$). For the single-crystal data collection, a suitable crystal was carefully selected and glued on a glass fiber. The X-ray data were recorded at room temperature on a Bruker SMART three-circle diffractometer with a CCD bidimensional detector (monochromatized Mo Kα radiation). The crystal-to-detector distance was 45 mm, allowing for a data collection up to 60° (2θ). Slightly more than one hemisphere of data was recorded. Crystal data and details of the data collection are given for both groups I-43m and P-43n in Tables 1 and 2. An empirical absorption correction was applied using the SADABS program[15] based on the method of Blessing.[16] The structure was solved by direct methods in the cubic space groups I-43m ($n°$ 217) and P-43n ($n°$ 218), and refined by full-matrix least squares using the SHELX-TL package.[17] Metal atoms were first located, and other non-hydrogen atoms were then placed from the subsequent Fourier syntheses. One of two crystallographically inequivalent carbon atom sites (labeled C1) is split on two positions each with an occupancy

(12) Flanigen, E. M.; Lok, B. M.; Patton, R. L.; Wilson, S. T. *Stud. Surf. Sci. Catal.* **1986**, *28*, 103.

(13) Bu, X.; Feng, P.; Stucky, G. D. *Science* **1997**, *278*, 2080.

(14) (a) Gier, T. E.; Stucky, G. D. *Nature* **1991**, *349*, 508. (b) Rao, C. N. R.; Natarajan, S.; Neeraj, S. *J. Am. Chem. Soc.* **2000**, *122*, 2810 and references therein.

(15) Sheldrick, G. M. SADABS, a program for the Siemens Area Detector ABSsorption correction, University of Göttingen, 1995.

(16) Blessing, R. *Acta Crystallogr.* **1995**, *A51*, 33.

(17) Sheldrick, G. M. SHELXTL version 5.03, sofware package for the Crystal Structure Determination, University of Göttingen, 1994.

Table 1. Crystal Data and Structure Refinement for $Zn_3Al_6(PO_4)_{12}$, 4*tren*, $17H_2O$ (MIL-74) (Specific Refinement Data for *P-43n* Are Given in Italics)

identification code	MIL-74
empirical formula	$C_{24}H_{118}Al_6N_{16}O_{65}P_{12}Zn_3$
formula weight	2400.97
temperature	293(2) K
wavelength	0.71073 Å
crystal system, space group	cubic, *I-43m* (*P-43n*)
unit cell dimensions	$a = 16.7942(1)$ Å
volume	4736.72(5) A^3
Z, calculated density	2, 1.683 Mg/m^3
absorption coefficient	1.125 mm^{-1}
$F(000)$	2484
crystal size	$0.24 \times 0.24 \times 0.24$ mm
θ range for data collection	1.71–29.75°
limiting indices	$-22 \leq h \leq 23$, $-23 \leq k \leq 23$, $-13 \leq l \leq 22$
reflections collected/unique	16 637/1247 [R(int) = 0.0286]
	29 988/2198 [R(int) = 0.0334]
completeness to $\theta = 29.75$	98.0%
absorption correction	none
refinement method	full-matrix least-squares on F^2
data/restraints/parameters	1247/0/65
	2198/0/105
goodness-of-fit on F^2	1.203
	1.176
final R indices [$I > 2\sigma(I)$]	$R1^a = 0.0321$, $wR2^b = 0.0954$
	$R1^a = 0.0404$, $wR2^b = 0.1014$
R indices (all data)	$R1^a = 0.0325$, $wR2^b = 0.0957$
	$R1^a = 0.0532$, $wR2^b = 0.1091$
absolute structure parameter	0.04(2)
largest diff. peak and hole	0.716 and -0.580 e Å^{-3}
	0.614 and -0.368 e Å^{-3}

^{a} R1 $= \sum||F_o| - |F_c||/\sum|F_o|$. ^{b} wR2 $= \{\sum[w(|F_o|^2 - |F_c|^2)^2]/\sum[w(|F_o|^2)^2]\}^{1/2}$, $w = 1/[\sigma^2(F_o^2) + (0.0618P)^2 + 2.599P]$ and $w = 1/[\sigma^2(F_o^2) + (0.0526P)^2 + 2.57P]$, where $P = [(F_o^2) + 2F_c^2]/3$.

Table 2. Comparison of the Refinements of $Zn_3Al_6(PO_4)_{12}$, 4*tren*, $17H_2O$ (MIL-74) in the Space Groups *I-43m* ($n°$ 217) and *P-43n* ($n°$ 218)^a

	I-43m hkl: h + k + l = 2n (0kl: k + l = 2n) hhl: l = 2n (h00: h = 2n)			*P-43n* hkl: no 0kl: no hhl: l = 2n h00: h = 2n		
	A	B	C	A	B	C
refl. meas	1229	1247	1242	1686	2198	2193
no. param.	65	65	65	103	103	103
R1	3.11%	3.15%	3.03%	4.03%	5.31%	5.22%
wR2	9.48%	9.54%	9.36%	10.51%	11.46%	11.40%
%Al on Al1 (6b in both)	100%	100%	100%	100%	100%	100%
Al1–O (Å)	1.752(2)	1.752(2)	1.751(2)	1.753(3)	1.755(3)	1.753(3)
%Al on Al2 (12d in *I-43m*) (6c in *P-43n*)	59%	59%	58%	63%	63%	64%
Al2–O (Å)	1.820(2)	1.820(2)	1.820(2)	1.780(3)	1.779(3)	1.779(3)
%Al on Al3 (6d in *P-43n*)				54%	54%	53%
Al3–O (Å)				1.849(3)	1.849(3)	1.848(3)

^{a} A, $I > 2\sigma(I)$; B, all data ($I > \sigma(I)$); C, all data + suppression of the worst F_o/F_c.

factor of 50%. The refinements took into account the positions of non-hydrogen atoms, the possibilities of Zn–Al repartition, and occupancies of the aluminum sites. Results will be discussed below. Table 2 compares the results obtained in both groups for different values of $I/\sigma(I)$, with reliability factors and corresponding Al–O distances which will be discussed in the following. The final refinements include the occupancy factors of 50% for the Zn/Al site 2 (in *I-43m*) or the Zn/Al sites 2a and 2b (in *P-43n*), in agreement with the Al/Zn ratio of 2 given by the chemical analysis. The corresponding reliability factors converge to R1 = 0.0321, wR2 = 0.0954 (for 1229 reflections $I > 2\sigma$ (I) and 65

Table 3. Atomic Coordinates and Equivalent Isotropic Displacement Parameters (Å$^2 \times 10^3$) for $Zn_3Al_6(PO_4)_{12}$, 4*tren*, $17H_2O$ (MIL-74)^a

	Wyckoff	x	y	z	U(eq)
		I-43m			
Al(1)	6b	0	1/2	1/2	13(1)
Al(2)^b	12d	0	1/2	1/4	17(1)
Zn(2)^b	12d	0	1/2	1/4	17(1)
P	24g	0.0645(1)	0.6225(1)	0.3775(1)	17(1)
O(1)	24g	0.1487(1)	0.6445(1)	0.3555(1)	34(1)
O(2)	48h	0.0165(1)	0.5919(1)	0.3054(1)	30(1)
O(3)	24g	0.0647(1)	0.5578(1)	0.4422(1)	28(1)
N(1)	8c	0.1978(2)	0.8023(2)	0.1978(2)	24(1)
C(1)^b	48h	0.1758(3)	0.8747(3)	0.2425(3)	33(1)
C(2)	24g	$-0.1749(2)$	0.6416(2)	0.3584(2)	36(1)
N(2)	24g	0.1945(1)	0.6276(2)	0.1945(1)	32(1)
O(1W)	2a	0	0	0	102(6)
O(2W)	8c	$-0.0944(4)$	0.9056(4)	0.0944(4)	101(3)
O(3W)	24g	0.2591(4)	0.5544(5)	0.4456(5)	253(8)
		P-43n			
Al(1)	6b	0	1/2	0	14(1)
Al(2)^b	6c	1/4	1/2	0	19(1)
Zn(2)^b	6c	1/4	1/2	0	19(1)
Al(3)^b	6d	0	1/2	1/4	12(1)
Zn(3)^b	6d	0	1/2	1/4	12(1)
P	24i	0.1229(1)	0.4355(1)	0.1222(1)	18(1)
O(1)	24i	0.1460(1)	0.3513(1)	0.1430(2)	36(1)
O(2)	24i	0.1947(1)	0.4840(1)	0.0901(2)	31(1)
O(2A)	24i	0.0934(1)	0.4832(1)	0.1945(1)	32(1)
O(3)	24i	0.0576(1)	0.5646(1)	$-0.0579(1)$	30(1)
N(1)	8e	0.3022(2)	0.3022(2)	0.3022(2)	26(1)
C(1)^b	24i	0.3237(6)	0.2583(5)	0.3749(5)	53(2)
C(1A)^b	24i	0.3743(3)	0.2570(3)	0.3242(3)	22(1)
C(2)	24i	0.1408(2)	0.6752(2)	0.1422(2)	38(1)
N(2)	24i	0.1276(2)	0.3065(2)	0.3045(2)	34(1)
O(1W)	2a	1/2	1/2	1/2	111(6)
O(2W)	8e	0.5936(4)	0.5936(4)	0.5936(4)	105(3)
O(3W)	24i	0.5484(5)	0.5578(5)	0.7415(4)	237(6)

^{a} U(eq) is defined as one-third of the trace of the orthogonalized U_{ij} tensor. ^{b} Occupancy factor fixed at 50%.

parameters) in *I-43m* and R1 = 0.0404, wR2 = 0.1014 (for 1686 reflections $I > 2\sigma(I)$ and 105 parameters) in *P-43n*. Atomic coordinates and isotropic displacement parameters are given in Table 3 for the *I-43m* and *P-43n* space groups.

Solid-State NMR. ^{27}Al and ^{31}P NMR spectra were acquired on a DSX 500 Bruker spectrometer with a magnetic field of 11.7 T. Bruker MAS probes of 4 and 2.5 mm rotor diameter were used for the different experiments. MAS simple pulse spectra, as well as RFDR and C7 double quantum experiments for ^{31}P, and 3QMAS for ^{27}Al, were acquired. The detailed experimental conditions for each experiment are detailed in the respective figure captions. Simulations of spectra were performed using Winfit.[26] Quantification of ^{31}P was directly performed on the MAS spectrum. For ^{27}Al, iteration between the 3QMAS and the MAS spectrum allowed one to obtain the best quantitative estimates.

Results and Discussion

Formulation of the Problem. The X-ray powder pattern (Figure 2) can be indexed in a cubic cell with $a = 16.794(1)$ Å. At first glance, the diagram can be indexed in an I centered lattice, but a very weak reflection, indexable in the same cell

(18) (a) Férey, G.; Taulelle, F.; Loiseau, T.; Lacorre, P. *J. Solid State Chem.* **1993**, *105*, 179. (b) Taulelle, F.; Loiseau, T.; Maquet, J.; Livage, J.; Férey, G. *J. Solid State Chem.* **1993**, *105*, 191. (c) Taulelle, F.; Pruski, M.; Amoureux, J. P.; Lang, D.; Bailly, C.; Huguenard, C.; Haouas, M.; Gérardin, C.; Loiseau, T.; Férey, G. *J. Am. Chem. Soc.* **1999**, *121*, 12148. (d) Taulelle, F.; Samoson, A.; Loiseau, T.; Férey, G. *J. Phys. Chem. B* **1998**, *102*, 8588.
(19) Baerlocher, C.; Meier, W. M.; Olson, D. H. *Atlas of Zeolite Framework Types*, 5th ed.; Elsevier Science B. V.: New York, 2001.
(20) Henry, M.; Beitone, L.; Taulelle, F.; Loiseau, T.; Férey, G. *Chem.-Eur. J.*, submitted.
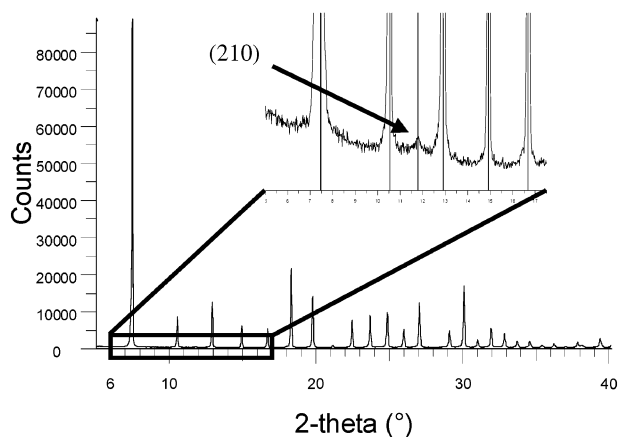
Figure 2. X-ray powder pattern of $Zn_3Al_6(PO_4)_{12}$, 4*tren*, 17H_2O (MIL-74) (λ: Cu Kα). The inset shows the (210) Bragg peak characteristic of *P*-43*n* symmetry, but absent in *I*-43*m* symmetry.

as (210), could rule out the I condition. The space group is *I*-43*m* (n° 217) if the weak reflection is not taken into account, but *P*-43*n* (n° 218) if it is. This ambiguity is at the origin of the present study. Indeed, theoretically, either this weak peak belongs to a byproduct and the space group is *I*-43*m* or, although extremely weak, it belongs to the main product and the space group will change into *P*-43*n*. A likely origin of this reflection is the onset, even partial, of cationic order. Such a tiny contribution requires a careful study of the problem, using not only X-ray diffraction, which is very dependent on the quality of the crystal, but the combination with solid-state NMR, which is a more local probe and can provide complementary information. We have shown the richness of information obtainable from the combined approach for some years.[18] It is worth noting that high-resolution electron microscopy could have been an accurate tool for discriminating between the two space groups, but, unfortunately, the crystals are destroyed immediately under the beam, even before the end of a diffraction experiment.

Information from the X-ray Structure Determination. Even after ψ-scans, the collection of data confirms the existence of the (210) reflection but with such a small intensity (background before, 0.6; intensity measured, 1.3; background after, 0.6) that it is not taken into account using standard procedures ($I > 2\sigma(I)$). With the latter, the structure can be solved in both groups (Tables 1 and 2) with the same topology, which will be described in detail below. Whatever the value of the $I/\sigma(I)$ criterion, the reliability factor is better for *I*-43*m* than for *P*-43*n*, but the number of data and of variable parameters is different.

From a crystal-chemistry point of view, the structure provides a good illustration of the scale chemistry concept. It can be described as a super-sodalite framework with aluminum, zinc,

(21) Xu, Y.-H.; Zhang, B.-G.; Chen, X.-F.; Liu, S.-H.; Duan, C.-Y.; You, X.-Z. *J. Solid State Chem.* **1999**, *145*, 220.
(22) Brunner, G. O.; Meier, W. M. *Nature(London)* **1989**, *337*, 146.
(23) Cheetham, A. K.; Fjellvåg, H.; Gier, T. E.; Kongshaug, K. O.; Lillerud, K. P.; Stucky; G. D. In *Zeolite and Mesoporous Materials at the Dawn of the 21st Century*; Galarneau, A., Di Renzo, F., Fajula, F., Vedrine, J., Eds.; Elsevier: New York, 2001; *Stud. Surf. Sci. Catal.* **2001**, *135*, 158 (05-O-05).
(24) Harrison, W. T. A.; Hannooman, L. *Angew. Chem., Int. Ed. Engl.* **1997**, *36*, 640.
(25) (a) Nenoff, T. M.; Harrison, W. T. A.; Gier, T. E.; Stucky, G. D. *J. Am. Chem. Soc.* **1991**, *113*, 378. (b) Wiebcke, M. *Microporous Mesoporous Mater.* **2002**, *54*, 331.
(26) Massiot, D.; Fayon, F.; Capron, M.; King, I.; Le Calvé, S.; Alonso, B.; Durand, J.-O.; Bujoli, B.; Gan, Z.; Hoatson, G. *Magn. Reson. Chem.* **2002**, *40*, 70.
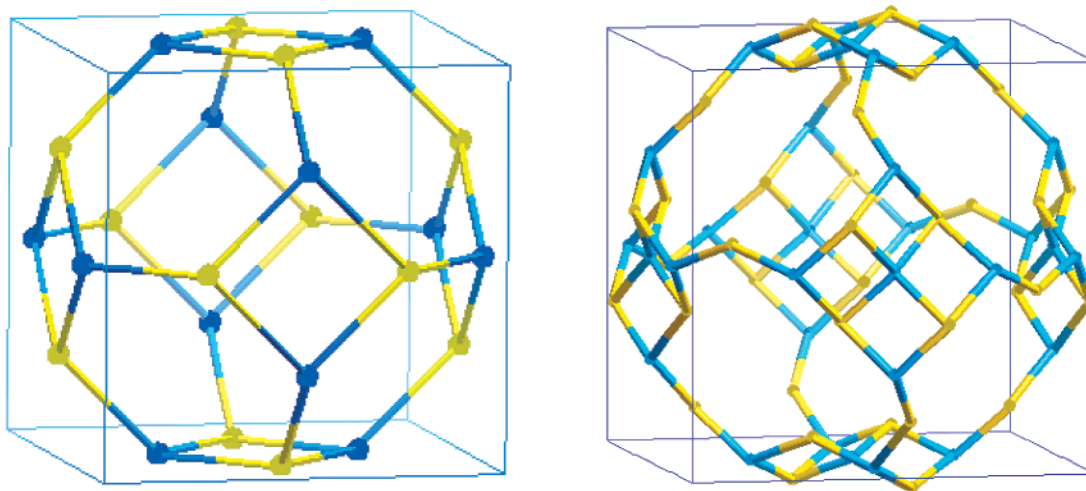
and phosphorus in tetrahedral coordination (Figure 3), in agreement with what was expected in the Introduction. The square faces of the truncated octahedron of the simple sodalite[19] (SOD) cage are replaced by faces with four squares in Zn_3Al_6-$(PO_4)_{12}$, 4*tren*, 17H_2O. This creates 12-membered ring windows instead of the hexagonal windows. These "large" windows (which have a free aperture of only 2.1 Å because some vertices of PO_4 tetrahedra point toward the center of this window) are blocked (Figure 4) by the protonated *tren* species which are disordered over two positions and exhibit the usual C–C and C–N distances. The TO_4 tetrahedra (T = Al or Zn) share all of their corners with the PO_4 tetrahedra, leading to the strict T–O–P alternation usually encountered in the AlPO-type materials. However, one of the oxygen atoms (O1) linked to the phosphorus is terminal and interacts through hydrogen bonds to the terminal nitrogen atom (N2) of each branch of the *tren* molecule. Its P–O distance (1.508(2) Å) is shorter than those engaged in the P–O–T linkages (P–O2 = 1.543(2) Å and P–O3 = 1.537(2) Å). The organic species is located at the center of the 12-ring window in such a way that the terminal oxygen of the phosphate group is hydrogen bonded with two nitrogen atoms N2 (P–O1⋯N2 = 2.825(3) Å). A hydrogen bond interaction also occurs between the terminal oxygen O1 and one of the water molecules (O3W) trapped inside the super-sodalite cage (O1⋯O3W = 2.833(8) Å). The terminal nitrogen N2 is hydrogen bonded to the oxygen O2 (2.971(3) Å). Each terminal nitrogen atom (N2) of the tripod-type tetraamine is protonated because the central nitrogen (N1) is not. This fact is in good agreement with the contrast observed for the pK_a values in such a branched amine molecule. The central nitrogen is protonated in very acidic medium only (pK_a < 2), and the external NH_2 groups are easily protonated in the presence of small amounts of acid (p$K_a \approx$ 9–10). The triprotonated *tren* species $[N_4C_6H_{21}]^{3+}$ ensures the electroneutrality of the structure because the inorganic framework has three negative charges $[Zn_3Al_6(PO_4)_{12}]^{3-}$.

The super-sodalite cavity with dimensions of 10 Å (measured between oxygen centers using an ionic radius of 1.35 Å) is occupied by a very strange cluster with 17 strongly bonded water molecules (O–O in the range 2.50–2.75 Å) which can be described as a centered tetrahedron, the six edges of which are decorated by two other water molecules. The compactness of this cluster is higher than that of all known varieties of ice and will be studied in greater detail in another paper.[20] The three-dimensional architecture of MIL-74 was previously described,[21] but neither the formula of the corresponding compound nor the protonation of the amines was correct.

The other most remarkable feature is the low value of the framework density (FD) of the MIL-74 topology. It is defined as the number of tetrahedral cations T per 1000 Å³. The search for solids with low framework densities is of particular interest in the field of synthesis of porous compounds. Brunner and Meier[22] established a relationship between the openness of a framework (or FD) and the size of the ring of the secondary building unit. It is assumed that structures containing 3-ring subunits will have a large pore volume. For example, the beryllosilicate[23] $K_{24}Be_{12}Si_{25}O_{74}\cdot96H_2O$ (OSB-2; FD = 12.7), built up from 3-ring units only, agrees with this concept. The FD value of the super-sodalite structure MIL-74 equals 8.9. To our knowledge, it is the lowest number observed so far for any

Figure 3. Perspective view of (top) a sodalite structure described either as a metal subnetwork or as connected tetrahedra, and (bottom), in the same way, the super-sodalite structure of $Zn_3Al_6(PO_4)_{12}$, 4*tren*, $17H_2O$ (MIL-74). Aluminum atoms are in blue, and phosphorus atoms are in yellow.

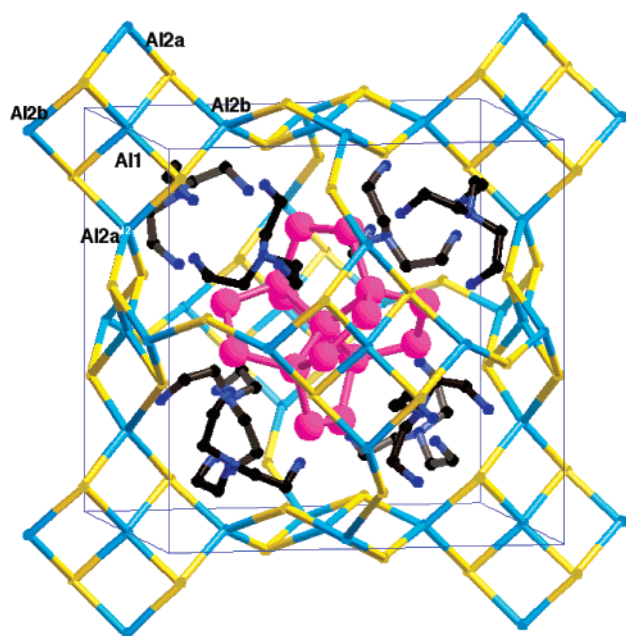**Figure 4.** The super-sodalite cage of $Zn_3Al_6(PO_4)_{12}$, 4*tren*, $17H_2O$ (MIL-74) with the *tren* moieties (carbon, black; nitrogen, dark blue) which block the 12-membered ring windows and the cluster with 17 H_2O (purple) molecules in the center of the cage.

Figure 5. Representation of the enneameric unit T_5P_4 (T = Al, Zn) and the *tren* molecule in MIL-74. The sites Al2a (6c) and Al2b (6d) correspond to one crystallographic position (noted Al2, 12d) in *I-43m*. Aluminum atoms are in blue, phosphorus atoms are in yellow, and oxygen atoms are in red.

microporous inorganic compound based on TO_4 tetrahedral units. Other solids exhibiting low FD values include the zinc phosphate[24] $ZnH_3(PO_4)_2 \cdot N(CH_3)_4$ (10.1) or gallium phosphate cloverite[10] (11.1). Both materials possess an interrupted framework as MIL-74. FDs of fully connected, TO_4-based networks are higher, for example, 12.7 for the zeolite faujasite[19] (FAU) and 12.1 for the phosphate UCSB-10[13] (SBT).

The building block of the MIL-74 structure is an enneameric unit containing five TO_4 (T = Al, Zn) and four PO_4 tetrahedra sharing vertices (Figure 5). In both cases, P occupies a single crystallographic site (24g) in *I-43m* and 24i in *P-43n*. In *I-43m*, there are two aluminum sites: the central aluminum of the enneamer Al1 (6b; noted site **1**) and the outer sites Al2 (12d; noted site **2**). In *P-43n*, there are three sites: Al1 (6b; site **1**), always central, Al2 (6c, noted site **2a**), and Al3 (6d, noted site **2b**), both peripheral. It is the main difference between the two
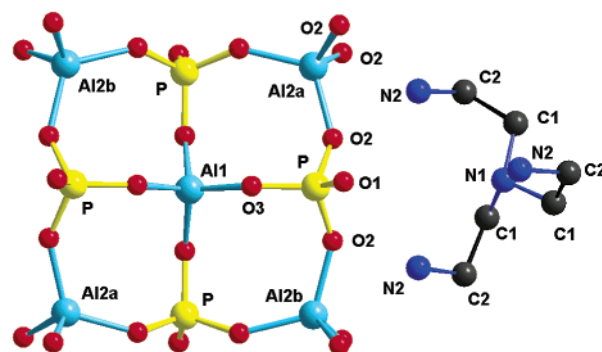
space groups. All of the other atoms of the structure have the same multiplicity in both groups, except oxygen O2 and carbon C1, which occupy the general position 48h in *I-43m* but two general positions 24i (labeled O2/O2A and C1/C1A) in *P-43n*. The problem to be addressed is the distribution of Zn and Al over sites Al1, Al2, and Al3. To take into account the maximum number of reflections in the structure refinement, the selection criterion became $I/\sigma(I) = 1$ for both space groups, and the occupancy factors on the aluminum sites were allowed to vary during the calculations. The first important result is that, whatever the space group, refinements converge to full occupancy of the Al1 site by aluminum (Table 2). In *I-43m*, the refinement gives an occupancy of 59% by aluminum on the Al2 site. The calculations in *P-43n* show a tendency to put more zinc (46%) in the Al3 sites (**2b**) than in the Al2 sites (**2a**) (37%). The observed Al/Zn distances also reflect this tendency. As compared to the pure Al–O distance at the Al1 site (1.751(2) and 1.752(2) Å), the distances for the other sites are larger (1.822(2) Å in *I-43m* and 1.794(2) and 1.851(2) Å in *P-43n* for Al2 and Al3, respectively). However, these T–O distances values are much smaller than those reported in zinc phosphates with sodalite[25a] (Zn–O = 1.946 Å) or interrupted sodalite-type[25b] frameworks (Zn–O = 1.934–1.937 Å). The small difference in distances in space group *P-43n* could explain the existence of the very weak (210) reflection on the powder
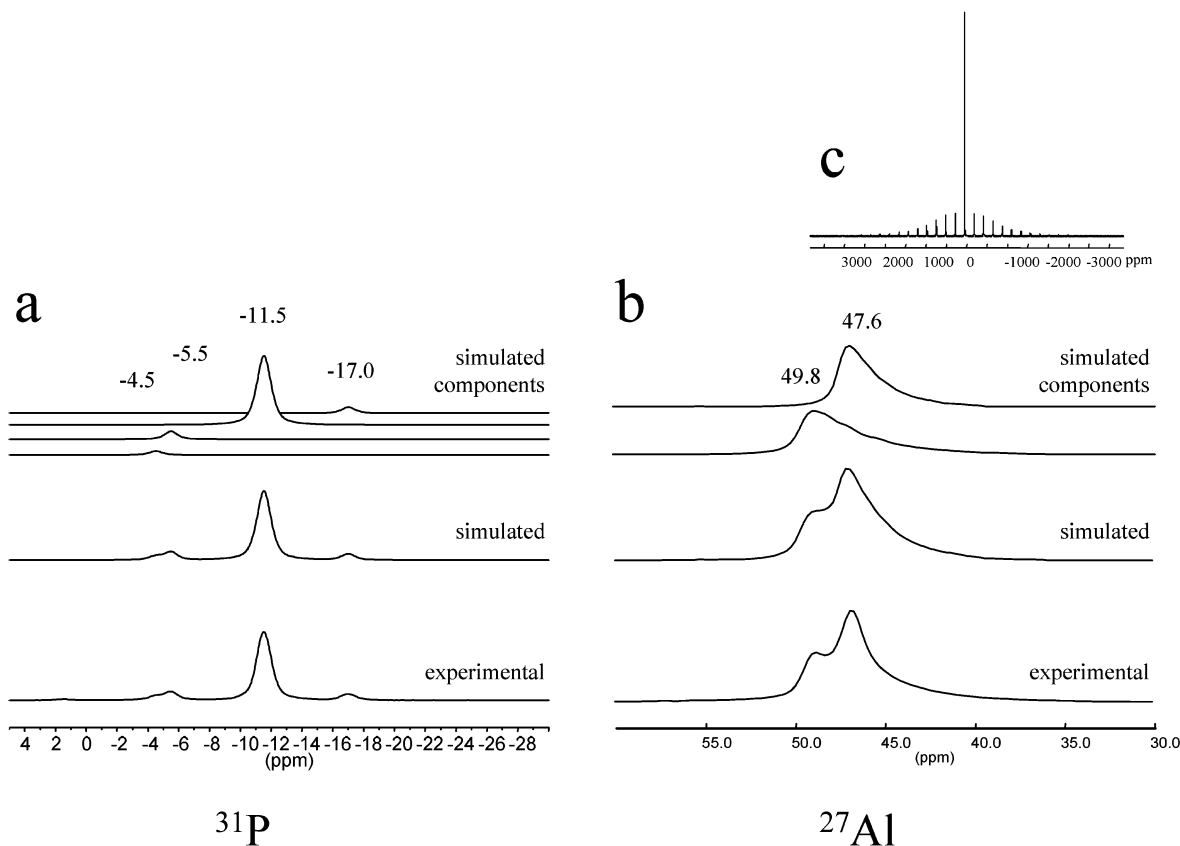
Figure 6. MAS spectra of $Zn_3Al_6(PO_4)_{12}$, 4*tren*, $17H_2O$ (MIL-74): (a) ^{31}P MAS at 10 kHz, with experimental, total simulation, and simulated components; recycle time of 2 min, slightly above 5*T1 after a 90° pulse. Chemical shift reference (0 ppm) is H_3PO_4, 85%. (b) ^{27}Al at 30 kHz, central transition isotropic lines with experimental, total simulation, and simulated components. (c) Full spectral width (1 MHz) of the ^{27}Al MAS spectrum. A radio frequency field of 45 kHz has been applied, with a recycle time of 1 s. Chemical shift reference (0 ppm) is $Al(NO_3)_3$ in nitric aqueous solution.

pattern, but it is clear that one reaches the limits of accuracy of the X-ray technique, even in hypothesizing a perfect crystal, which is rarely true. It is, however, likely that solid-state NMR, a more local probe, could provide a more accurate description of the order within the enneameric building block.

Information from NMR and Discussion. MAS spectra of ^{31}P and of ^{27}Al are displayed with their simulations in Figure 6. The ^{31}P spectrum exhibits one main line at -11.5 ppm with 81% intensity and three additional lines at -17, -5.5, and -4.5 ppm with, respectively, 6.6%, 8.1%, and 4.3% intensity. The ^{27}Al spectrum exhibits two components at 48 and 50 ppm. Both lines are in the tetrahedral range of chemical shifts, and these sites are therefore assigned to that coordination state.

Actually, a unique phosphorus crystallographic site is present in both space groups: 24g in *I-43m* and 24i in *P-43n*. The three sites surrounding each phosphorus atom are a central site **1** (6b) and two sites **2** (12d) for *I-43m*, and a central site **1** (6b) surrounded by two peripheral sites **2a** (6c) and **2b** (6d) for *P-43n*.

The overall stoichiometry $Zn_3Al_6P_{12}$ of the framework would be compatible with a central site **1** fully occupied with Al, and two peripheral sites **2** (12d) shared between Al and Zn (50:50) for *I-43m*, or sites **2a** (6c) and **2b** (6d) fully occupied by either Al or Zn for *P-43n*. The XRD results suggest some distribution of Al and Zn on site **2** (*I-43m*) or on sites **2a** and **2b** (*P-43n*). Full occupancy by aluminum is expected on site **1** in both choices as the average ⟨Al−O⟩ distance found for this site is 1.75 Å as is expected for a four coordinated aluminum site.

What follows from ^{31}P NMR? If the small peaks are neglected, a single phosphorus line remains, consistent with a fully ordered situation (*P-43n*) and therefore full occupancy of site **1** (6b) by Al, site **2a** (6c) by Al, and site **2b** (6d) by Zn. However, two problems arise. First, the additional components are weak but not unimportant ($\sim$20% together) and may pertain to the actual phase under study rather than to impurities. Second, the two signals in the aluminum spectrum exhibit line shapes which suggest some distribution in their surroundings. These two observations are in good agreement with the *I-43m* choice. A definite quadrupolar second-order line shape with well-defined discontinuities would have been a strong hint for a *P-43n* choice. If both observations can be related to a pure phase, then the provisional choice of *P-43n* may be reasonably questioned.

Two additional experiments including RFDR and double quantum were performed on ^{31}P NMR. The first correlates phosphorus sites with dipolar coupling, that is, sites at most a few angstroms apart. With a very long mixing time (a few hundred milliseconds), every phosphorus atom of the phase must be correlated to another. The process is driven by spin diffusion of phosphorus between them and probably also relayed by the hydrogen of the templating agents. The second experiment provides the same type of information, but with the short mixing time used, and the absence of dipolar spin diffusion, the double quanta experiment senses an even shorter range of proximities.

The results of both experiments are plotted in Figure 7. The RFDR shows that cross-peaks between each pair of lines exist, demonstrating clearly that all lines in the ^{31}P spectrum are
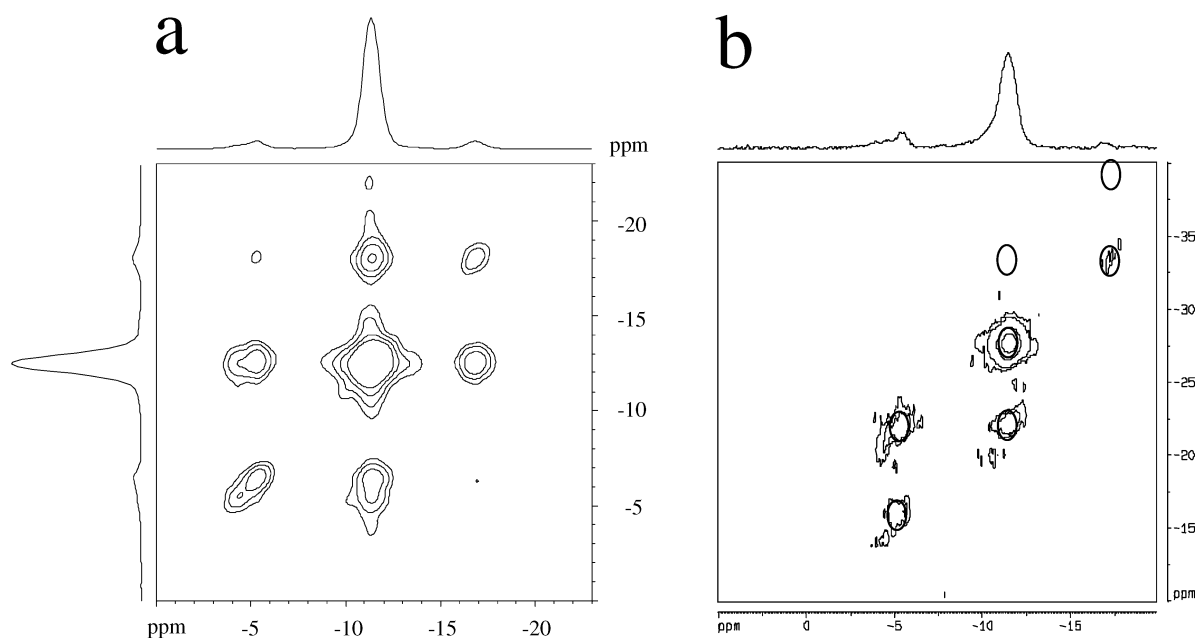
Figure 7. ^{31}P 2D spectra of $Zn_3Al_6(PO_4)_{12}$, 4*tren*, 17H_2O (MIL-74): (a) RFDR with MAS rotation of 12.5 kHz, a mixing time of 1200 rotation periods (96 ms), 16 accumulated FID per *t*1 and 128 *t*1, a *t*1 increment of 80 μs, acquisition mode in TPPI, 12.5 kHz in *t*2 dimension. Radio frequency field: 70 kHz. Recycle time is 1 min with a presaturation scheme to allow for faster experiment. Total experimental time: 69 h 15 min. (b) DQ (DQ) ovals corresponding to the expected cross-peaks have been superimposed to the contour plot; only two cross-peaks present in RFDR are missing due to the weak signal-to-noise ratio. The pulse sequence is from ref 34. RF field: 87 kHz and MAS rotation 12.5 kHz. Excitation and reconversion time of the C7 blocks were of six rotation periods (322 μs), with 104 accumulated FID per *t*1, and 64 *t*1 with 50 μs increment acquisition mode in TPPI, and 12.5 kHz in *t*2 dimension. Recycle time is 1 min with a presaturation scheme to allow for faster experiment. Total experimental time: 98 h 40 min.

dipolarly coupled to each other. They therefore all belong to the same phase. The DQ experiment used a C7 series of cycles to excite the double quanta, in principle, a quite efficient method. The coupling between all phosphorus lines is still there, albeit a little less contrasted, due to a lower signal-to-noise ratio for that experiment as compared to the RFDR. These results lead to the conclusion that the single phosphorus site in the case of *P*-43*n* does not strictly apply and that some distribution of phosphorus occurs in the sample.

Therefore, aluminum NMR was considered anew. A 3QMAS experiment allowed one to obtain higher resolution, correlating the isotropic part of the spectrum to its anisotropic part.[27] This correlation is quite sensitive to the distribution of sites. Usually such a distribution leads to some distribution of the quadrupolar interaction, and for a fixed radio frequency field, the experiment weighs the different C_Q contributions differently, as Fernandez has exploited as a general technique in his MASAI[28] method. The 3QMAS experiment of Figure 8 exhibits two resolved components. Both sites are extracted as isotropic slices. The line shape of each site can therefore be simulated separately on these slices. Once done, the same line shapes are used for decomposing the MAS spectrum into two components. All line shape parameters except the amplitudes of the components are fixed. Once optimized, the area of each component is measured. The values obtained are for site **1** δ_{iso} = 49.74 ppm, C_Q = 1.6 MHz, η_Q = 0.4 and for site **2** δ_{iso} = 47.6 ppm, C_Q = 1.233 MHz, η_Q = 0.6. The respective integrated areas are 47% and 53% ($\pm$4%), very close to a 1:1 ratio.

Actually, the line shapes for the two aluminum sites are simulated as sums of quadrupolar second-order patterns, ac-

cording to a Czjzek distribution.[26,29] These individual line shapes characteristic of some site distribution can be simulated to describe the ^{27}Al MAS spectrum (Figure 6). It may appear inconsistent to have site **1** fully occupied by aluminum exhibiting a distribution line shape, of comparable width to site **2**. However, one must remember that the quadrupolar interaction senses differences in the environment quite far away from the site considered. If a distribution of Al and Zn is assumed on sites **2a** and **2b**, then Al**1** will reflect this distribution in its line shape.

The *P*-43*n* choice seems, therefore, not fully acceptable. The *I*-43*m* choice, with Al and Zn distributed on sites **2** only, leads to three situations, PAl**1**Al**2**Al**2** (statistical weight of 0.25), PAl**1**Al**2**Zn**2** (statistical weight of 0.50), and PAl**1**Zn**2**Zn**2** (statistical weight of 0.25), where the total ratio Al/Zn on site **2** remains equal to 1. If site **1** is also distributed, six situations for P exist, the three former and their equivalent with Al**1** replaced by Zn**1**.

The *P*-43*n* choice leads to only one environment if site **1** is fully occupied by Al, and both sites **2a** and **2b** are strictly ordered. If sites **2a** and **2b** are fully disordered, *P*-43*n* is completely equivalent to *I*-43*m*, with site **1** ordered. Yet one seems to observe by XRD only a partial disorder. If, in addition to sites **2a** and **2b** being disordered, the central site **1** is also disordered between Al and Zn, then the situations becomes equivalent to choice *I*-43*m* with the central site disordered, and six types of environments would be observed.

Two extreme situations may occur. First, a fully ordered site **1** with site **2** intrinsically disordered corresponds to *I*-43*m*. Second, a fully ordered site **1** with sites **2a** and **2b** fully ordered

(27) Frydman, L.; Harwood, J. S. *J. Am. Chem. Soc.* **1995**, *117*, 5367.
(28) Fernandez, C.; Pruski, M. *Stud. Surf. Sci. Catal.* **2001**, *135*, 2128.

(29) Czjzek, G.; Fink, J.; Götz, F.; Schmidt, H.; Coey, J. M.; Rebouillat, J.-P.; Liénard, A. *Phys. Rev. B* **1981**, *23*, 2513.
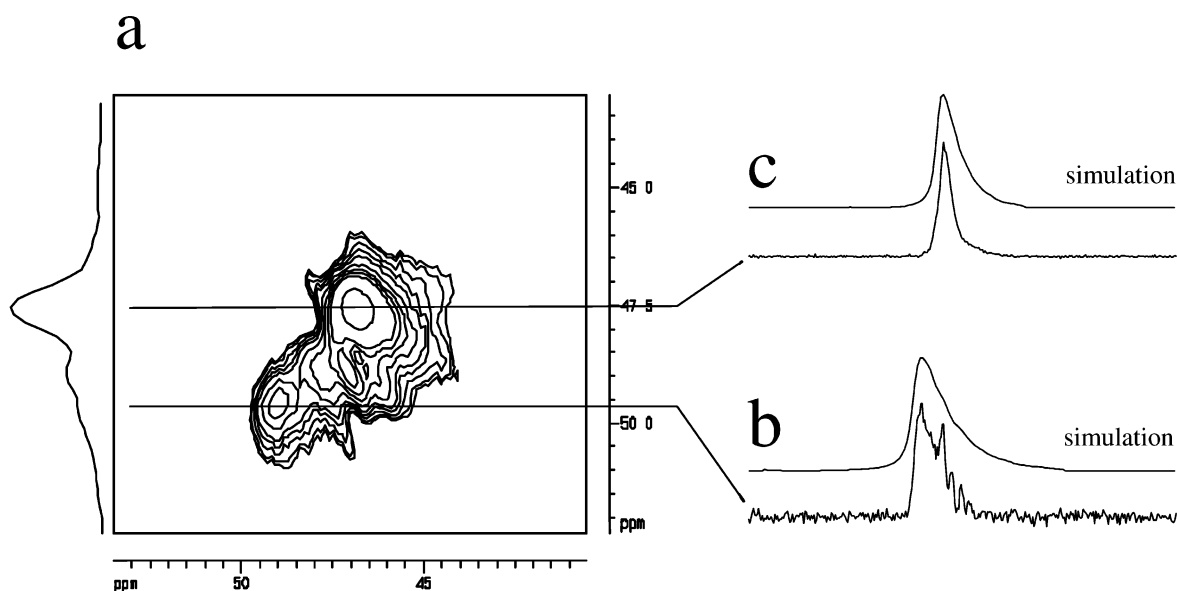
Figure 8. Al 3QMAS of $Zn_3Al_6(PO_4)_{12}$, 4*tren*, 17H_2O (MIL-74): (a) 3QMAS contour plot; (b) slice of the 49.6 ppm site and its simulation; (c) slice of the 47.4 ppm and its simulation.

corresponds to *P*-43*n*. These cases lead to three phosphorus environments in *I*-43*m* with an order on site **1**, and only one in *P*-43*n*. If Zn and Al are fully disordered over sites **1**, **2a**, and **2b**, the space group is *I*-43*m*, and six types of phosphorus environments are expected.

Actually, four lines are observed in phosphorus NMR. The most intense line can be assigned to the PAl**1**Al**2a**Zn**2b** environment, for it is the most probable statistical environment. Its intensity is 81%, quite close to the *P*-43*n* choice for which one expects 100%. The three additional lines can be assigned by analogy to assignment in aluminosilicates, where the chemical shift of silicon Q₄ sites is a function of the number of aluminums substituting for silicon in the second sphere of coordination. Each time a silicon atom is substituted by an aluminum atom, the chemical shift moves downfield with an increment of 4−6 ppm due to the difference in oxidation degree between silicon and aluminum. Therefore, the line at −17 ppm (8.35%) at higher field corresponds to PAl**1**Al**2a**Al**2b**, the main line at −11.5 ppm (81.7%) corresponds to PAl**1**Al**2a**Zn**2b**, and the two lines at −4.5 (2.9%) and −5.5 ppm (7.1%) correspond to PAl**1**Zn**2a**Zn**2b** or PZn**1**Al**2a**Zn**2b** environments. A signal corresponding to PZn**1**Al**2a**Al**2b** would be at about 1−2 ppm difference from the main signal at −11.5 ppm and would probably be resolved from it. Because no such signal is observed, the concentration of such an environment is below the threshold of detection, less than 1%. No signal is detected corresponding to PZn**1**Zn**2a**Zn**2b**.

The presence of these additional lines confirms the result from XRD analysis, that some disorder is indeed present in the structure. As the aluminum line shapes reflect these distributions, the conclusion is equally confirmed from ²⁷Al NMR. For quantification purposes, ³¹P is the most accurate probe. ²⁷Al NMR senses the distribution qualitatively on the line shape. By XRD, many attempts have been made to refine the structure with partial occupancy of site **1**, but they all lead to negligible amounts of zinc on site **1**. The best estimate of zinc in site **1** is given by the ³¹P signal of PZn**1**Al**2a**Zn**2b** of 2.9%, with less than 1% PZn**1**Al**2a**Al**2b** not detected by NMR.

Now, two situations can be considered. The structure is actually ordered as the *P*-43*n* choice supports, but not totally, or the structure is disordered as required by the *I*-43*m* choice, but not completely. There is no way to continuously vary a space group to take into account such a continuously variable situation.

Both choices provide a structure description that is acceptable, with very good reliability factors R1 (3.21% and 4.04%). However, this criterion of the *R* value does not constitute a quantitative descriptor of the relative quality of the two descriptions. To state more accurately whether one of the descriptions is more relevant than the other, one must resort to use a statistical test, for example, Hamilton's test.[30] This procedure compares the *R* values obtained with different constraints configurations (variation of number of adjustable parameters) for a given reflections data set. Yet, in our case, the structure may be described in two distinct space groups that are not in a group/subgroup relation, and the Hamilton's test cannot be applied for this specific problem. Therefore, no definite method can state which structural solution is best between both space group choices. Both structural solutions are provided in the CIF files given as the Supporting Information, because they are both topologically accurate and describe structurally well the compound considered.

Moreover, the intensities of specific reflections observed in *P*-43*n* can be estimated as a function of the Zn/Al ordering rate. A simulation of the intensity evolution for the (210) reflection was performed by using the PowderCell[31] software between two extreme situations: strict order, Al**2a**, 100%, Zn**2a**, 0%; Al**2b**, 0%, Zn**2b**, 100%; and complete disorder, Al**2a**, 50%, Zn**2a**, 50%; Al**2b**, 50%, Zn**2b**, 50%. The variation of the relative intensity of the (210) Bragg reflection follows a second-order polynomial formula: $I_{210} = 19x^2 - 19.854x + 5.1857$, where *x* is the zinc population in site 2b. This model shows that the relative intensity (210) is rather weak. For small values of Zn/Al ordering, the intensity of the (210) line changes slowly. It

(30) Hamilton, W. C. *Acta Crystallogr.* **1965**, *18*, 502.
(31) Kraus, W.; Nolze, G. PowderCell for windows, version 2.3, Berlin, Germany, 1999.

reaches 0.1% of the most intense Bragg peak (110) for a 60/40 ordering (Zn/Al) and 0.6% for a 70/30 ordering (Zn/Al) on the site **2b**. It reaches 4.33% for complete order (Al2a, 100%; Zn2b, 100%). This consideration indicates that it is only beyond 80/20 ordering that partial order on sites **2a** and **2b** can be reasonably detected by the presence of the (210) line in X-ray diffraction.

Phosphorus NMR probes the different environments expected for ordered and disordered sodalite or super-sodalite (a decorated sodalite in the sense of O'Keeffe[32]). From the RFDR and double quantum experiments, all phosphorus environments are neighbors (within dipolar distance) to any other phosphorus environment. The compound can, therefore, not be described as a superposition of homogeneous domains. It is definitely a homogeneous distribution of environments.

The amount of each phosphorus NMR component could be followed as a function of any parameter that is thought to play a role in changing their proportions. The kinetics of crystallization during hydrothermal synthesis may be the key factor for the Al/Zn ordering variation; alternatively, the proportion of each component is independent of the kinetic advance, indicating thermodynamic control of disorder. To validate this argument, different crystalline samples of MIL-74 were obtained, from hydrothermal syntheses at 180 °C for 1–5 weeks. An additional product was obtained by substituting the aluminum source from Aldrich (50–57% of Al_2O_3) by the Prolabo source (64.5–67% of Al_2O_3). The latter synthesis leads to large crystals and for an overall synthesis period of 5 weeks mimics the behavior of a much longer synthesis with the Aldrich source. All six samples were analyzed by solid-state ^{31}P NMR. The six ^{31}P NMR signatures are strictly identical. This observation shows that the Al/Zn ordering degree is not a kinetically governed parameter but is thermodynamically controlled.

What could therefore be the thermodynamical parameter controlling the Zn/Al distribution? A complete order of the super-sodalite would mean enneameric units having a Zn2b–Al1–Zn2b diagonal and a Al2a–Al1–Al2a diagonal of the supersquare. Because of the difference in Al–O and Zn–O distances (~1.75 Å/~1.93 Å), it would be extremely surprising to obtain equal diagonals of the enneameric unit. The diagonals of this unit are assumed to be equal to $a/2$ in both *I-43m* and *P-43n* space groups.

Actually, the crystal undergoes two contradictory demands to minimize its lattice free energy. First, full ordering between Zn and Al, alternating a degree of oxidation 2+ with a degree of oxidation 3+, minimizes the electrostatic energy, in full analogy to Lowenstein's rule in zeolites, a contribution to the enthalpic part of the lattice energy. Second, equalization of both diagonals in the enneameric units generates the axis of symmetry of order 4. A higher symmetry increases the entropy of the crystal, decreasing the lattice free energy of the crystal.[35] Minimizing both parts of the free energy cannot be made in the same geometry. The balance of both demands imposes some Al/Zn distribution for the different crystallographic sites. If the

enthalpic lattice energy is dominant, then *P-43n* would be observed, whereas *I-43m* would be obtained if the entropic lattice energy is dominant. If both are of the same order of magnitude, then an intermediate solution between both space groups must occur. Among all intermediate solutions, only one leads, the *P-43n* choice, to equalization of the supersquare diagonals, and this is the one experimentally observed.

Conclusion

A new phase of a mixed zinc–aluminum phosphate Zn_3Al_6-$(PO_4)_{12}$, 4*tren*, $17H_2O$ (MIL-74) has been obtained in this study. It exhibits a super-sodalite topology with the lowest framework density known. This super-sodalite topology has many facets: its ability to accommodate many divalent and monovalent cations[33] in the network, and an intriguing water cluster. In addition, the templating agents are not located inside the pores but belong to the framework. It is, therefore, a true intermediate compound between a classical aluminophosphate nanoporous material and a metal-organic framework,[34] but with cationic organic linkers instead of the classical anionic linkers.

The ordering of Zn and Al has been studied in detail by combining XRD and NMR. The "disorder" of this structure has been shown to be reproducible and thermodynamically controlled. This type of reproducible homogeneous distribution of atoms may be of utmost importance in the construction of periodic materials with reproducible deviation from perfect periodicity. This structural description allows one to reevaluate the previously published[21] analogue network topology where the chemical composition was wrong and therefore the problem of order/disorder and its relation to the framework formation was completely overlooked.

We believe that the above result is common to structural resolutions that XRD–NMR crystallography allows one to access. Not only are fine details of a better structural description grasped, but also order quantification is even reached. The symmetry chosen to describe the crystal structure, here, *I-43m* or *P-43n*, appears as a way to take into account the amount of information experimentally collected. The symmetry must be lowered here, from *I-43m* to *P-43n*, to accommodate the increased amount of information when adding to XRD the NMR results. At a given stage, the choices permitted by the 230 3D space groups are no longer sufficient. Additional information must be added in the crystal description, as some degree of Zn/Al distribution, but the crystal remains better described as being just between two space groups, with a thermodynamically ordered state of organization.

Supporting Information Available: CIF files obtained from the single-crystal refinement in *I-43m* and *P-43n* (PDF). This material is available free of charge via the Internet at http://pubs.acs.org.

(32) (a) O'Keeffe, M.; Hyde, B. G. *Crystal Structures. I. Patterns and Symmetry*; Mineralogical Society of America: Washington, DC, 1996; p 315. (b) O'Keeffe, M.; Eddaoudi, M.; Li, H.; Reineke, T.; Yaghi, O. M. *J. Solid State Chem.* **2000**, *152*, 3.
(33) Beitone, L.; Taulelle, F.; Loiseau, T.; Férey, G., manuscript in preparation.
(34) Eddaoudi, M.; Li, H.; Yaghi, O. *J. Am. Chem. Soc.* **2000**, *122*, 1391.
(35) Rosen, J. *Symmetry in Science: An Introduction to the General Theory*; Springer-Verlag: New York, 1995.

JA0294818